nature genetics

A conserved microRNA module exerts homeotic control over *Petunia hybrida* and *Antirrhinum majus* floral organ identity

Maria Cartolano[1], Rosa Castillo[1], Nadia Efremova[1], Markus Kuckenberg[1], Jan Zethof[2], Tom Gerats[2], Zsuzsanna Schwarz-Sommer[1] & Michiel Vandenbussche[2]

It is commonly thought that deep phylogenetic conservation of plant microRNAs (miRNAs) and their targets[1,2] indicates conserved regulatory functions. We show that the *blind* (*bl*) mutant of *Petunia hybrida*[3] and the *fistulata* (*fis*) mutant of *Antirrhinum majus*[4,5], which have similar homeotic phenotypes, are recessive alleles of two homologous miRNA-encoding genes. The *BL* and *FIS* genes control the spatial restriction of homeotic class C genes[6,7] to the inner floral whorls, but their ubiquitous early floral expression patterns are in contradiction with a potential role in patterning C gene expression. We provide genetic evidence for the unexpected function of the *MIRFIS* and *MIRBL* genes in the center of the flower and propose a dynamic mechanism underlying their regulatory role. Notably, *Arabidopsis thaliana*, a more distantly related species, also contains this miRNA module but does not seem to use it to confine early C gene expression to the center of the flower.

The spatial partitioning of floral homeotic gene expression is crucial for wild-type flower development. Several transcription factors participate in this control, which aims at transcriptional silencing of the so-called 'C genes' outside their genuine expression domain in the inner two whorls of the flower, where they govern reproductive organ (stamen and carpel) development[6,7]. The functions of orthologous repressor genes, constituting the A function of the floral ABCs[6], are, in part, comparable between different species[8], as are some of the *cis*-acting regulatory regions within the large second intron of their structurally and functionally related target C genes *AGAMOUS* (*AG*) in *Arabidopsis thaliana*[7], *pMADS3* in *P. hybrida*[9] and *PLENA* and *FARINELLI* (*PLE* and *FAR*) in *A. majus*[10]. There are also exceptions to these overall similarities among species. For instance, orthologs of the *A. thaliana APETALA2* (*AP2*) gene have no role in C gene regulation in *P. hybrida*[11] or *A. majus*[12], raising the question of whether other genes fulfill this role. Candidates are the *BL* gene in *P. hybrida* and *FIS* in *A. majus*, which, when mutated, show markedly similar homeotically converted stamenoid petals in their second floral whorls[4,5] (**Fig. 1**).

By a combination of transposon tagging and map-based cloning strategies, we cloned the *BL* and *FIS* genes and found that they encode homologous *bona fide* miRNAs (miRBL and miRFIS), related in their core sequences to members of the large miR169 family[13,14] (**Fig. 2**). The *bl*-1 and *fis*-1 alleles lie within large genomic deletions and thus represent null alleles; *bl*-2 and *fis*-2 are transposon induced and genetically unstable alleles (**Fig. 2a**). miRNA-encoding genes are relatively small targets for mutation, and therefore, recessive mutants are infrequent; *bl* and *fis* thus offer a rare opportunity to study and compare the function of potential orthologs in two plant species.

miRNAs control gene expression by recognizing short complementary sequences in their transcripts (miRNA-recognition elements, or MREs), which are then post-transcriptionally targeted for cleavage or translational inhibition. Computational analysis of species with sequenced genomes and experimental evidence suggests that miR169 targets members of the *NF-YA* (also known as *HAP2* or *CBF-B*) gene family[13,15]. We cloned and sequenced cDNAs encoding *P. hybrida* and snapdragon *NF-YA* family members (*PhYA* and *AmYA* cDNAs, respectively; **Supplementary Fig. 1** online) and found that they also contain an MRE for miRBL or miRFIS within their 3′ UTR (**Fig. 2d**). By criteria developed to determine the efficiency of target cleavage[16], such as the number and position of mismatches between miRNA and

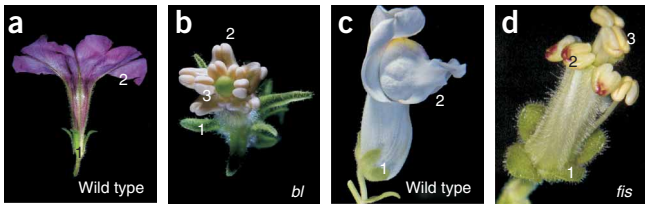

Figure 1 Phenotypes of mutant and wild-type flowers. (**a**,**b**) *P. hybrida*. (**c**,**d**) *A. majus*. **b** and **d** show homeotic conversion of petals to stamens in the *bl*-1 and *fis*-1 mutants. Whorls are numbered, and genotypes are indicated.

[1]Max Planck Institut für Züchtungsforschung, Plant Molecular Genetics Department, Carl-von-Linne-Weg 10, 50829 Köln, Germany. [2]Radboud University Nijmegen, Institute for Wetlands and Water Research, Plant Genetics Toernooiveld 1, 6525 ED Nijmegen, The Netherlands. Correspondence should be addressed to Z.S.-S. (schwarzs@mpiz-koeln.mpg.de).

Received 22 January; accepted 9 May; published online 24 June 2007; doi:10.1038/ng2056

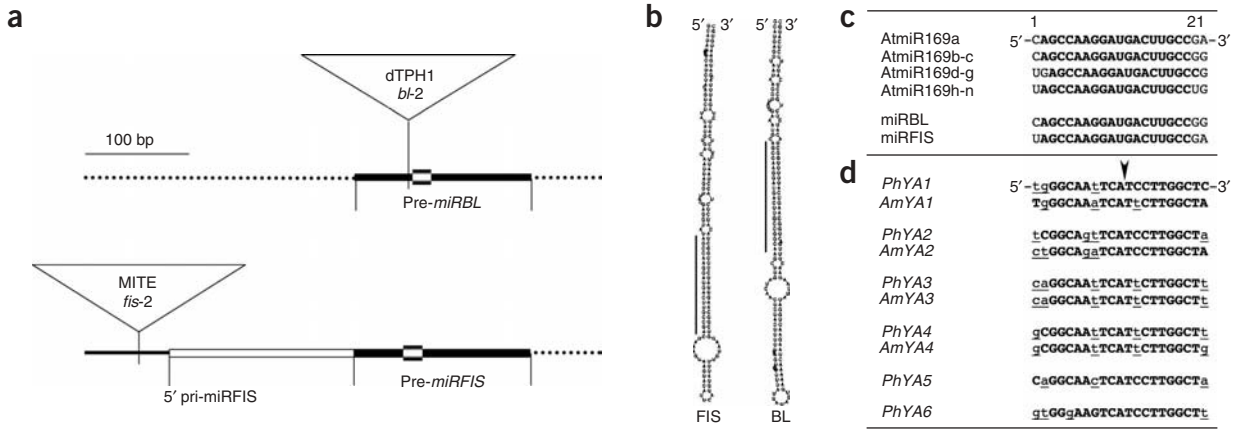

Figure 2 The BL and FIS miRNAs and their targets. (**a**) Structure of the genomic loci. Vertical lines show the position of transposons in the unstable alleles and the borders of substructures resulting from miRNA processing. The shaded box indicates the mature miRNA. (**b**) Stem-loop structure of the FIS and BL pre-miRNAs. Secondary structure calculations were done by the RNAfold program (http://rna.tbi.univie.ac.at/cgi-bin/RNAfold.cgi). The vertical lines show the positions of the mature miRNAs. (**c**) Sequence alignment of the mature miRNAs (AtmiR169 from ref. 14). The miRNA core sequence is in boldface. (**d**) Alignment of target sequences. Boldface upper-case letters indicate complementarity to the miRNA in *AmYA* and *PhYA* transcripts; mismatches between the miRNA and target sequences are lower case and underlined. The arrowhead indicates the 5′ end of the miRNA-mediated target cleavage product.

MRE, all MREs are potentially sensitive to miRNA-directed destruction. We detected the expected *NF-YA* cleavage products in *P. hybrida* and *A. majus* (**Supplementary Methods** and **Supplementary Table 1** online and **Fig. 2d**).

Most C genes contain two similarly spaced CCAAT boxes, the consensus *cis*-acting binding sites of *NF-YA*[10,17], in their second introns, and reporter gene expression studies in transgenic *A. thaliana* plants indicate that these CCAAT boxes are essential to enhance and maintain *AG* transcription[17]. Thus, ectopic expression of C genes in the *bl* and *fis* mutants is probably due to enhanced *NF-YA* expression in the outer whorls. This would imply that *BL* and *FIS* expression is confined to the outer whorls, complementary to that of *NF-YA* and the C genes in the inner whorls. We tested this prediction by *in situ* hybridization to detect the miRNAs (and *NF-YA* transcripts) in developing floral primordia. In conflict with the expected mutually exclusive expression patterns, the distribution of miRFIS and miRBL in young flowers is uniform throughout early development, even at stages when *PLE* (or pMADS3)[9] transcription is initiated in the center of the flower primordium (**Figs. 3a–d**). miRFIS and miRBL expression then decreases, first in the sepals (**Fig. 3e,f**) and then in petals and the central whorls as organs further differentiate (data not shown). Thus, it seems unlikely that miRBL and miRFIS function to clear *NF-YA* expression in the outer whorls while allowing the establishment and maintenance of C gene expression in the central C domain. Indeed, analogous to the ubiquitous expression of miRFIS, transcription of its potential *NF-YA* targets *in situ* overlaps with that of miRFIS (**Fig. 3g,h**). Furthermore, we could not detect changes in the pattern or level of *NF-YA* expression in the *fis* mutant by *in situ* hybridization (**Supplementary Fig. 2** online). Such 'incoherent coexpression' of miRNAs and their targets has been observed in both plants[2,18] and animals[19] and has been suggested to represent a fine-tuning mode to control target gene expression. Changes in target gene transcription or

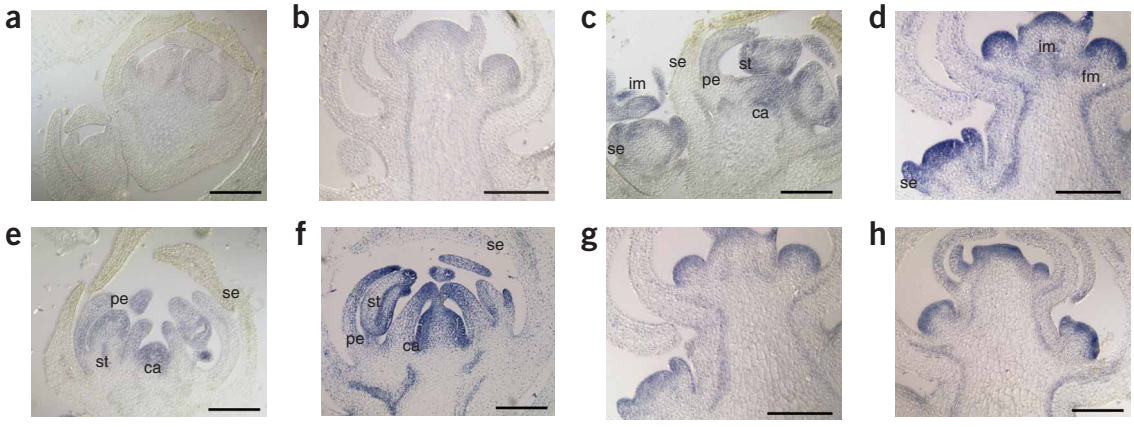

Figure 3 miRBL, miRFIS and *AmNF-YA* expression during early flower development. (**a–h**) *In situ* hybridizations with the miRBL (**a**,**c**,**e**) and miRFIS probes (**b**,**d**,**f–h**) on longitudinal sections of *P. hybrida* and *A. majus* inflorescences carrying young flower primordia at different developmental stages. miRNA expression is not detectable in the *bl*-1 and *fis*-1 mutants (**a**,**b**). The miRNAs are uniformly transcribed in young wild-type flowers (**c**,**d**), including the central region where C gene transcription initiates (see **Fig. 4b**). miRNA expression decays in the sepals and petals in differentiating wild-type flowers (**e**,**f**). *AmYA2* and *AmYA4* transcription in the wild type (**g**,**h**) overlap with miRFIS expression (**d**). The sections in **d** and **g** are serial. im, inflorescence meristem; fm, floral meristem; se, sepal; pe, petal; st, stamen; ca, carpel. Size bars = 200 μm.

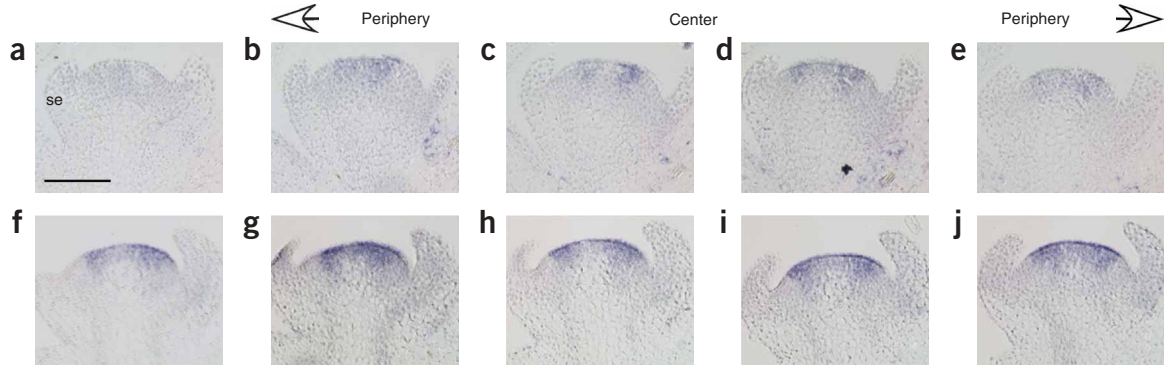

Figure 4 Enhanced *PLE* gene expression in the *A. majus fis*-1 mutant. (**a**–**j**) Longitudinal serial sections of wild-type (**a**–**e**) and *fis*-1 mutant (**f**–**j**) flowers, probed with antisense *PLE* RNA. The position of the sections in the flower primordium is indicated at the top. se, sepal; size bar = 100 μm.

translation are expected to be moderate in this case and are not easily quantifiable, in particular if target gene expression is under feedback regulation by the protein products of these very genes[16]. Nevertheless, quantitative RT-PCR, a more sensitive means of studying steady-state transcript levels compared with *in situ* analyses, suggests that *PhYA1* transcription is two to three times higher during later developmental stages in the *bl* mutant, whereas the other *PhYA* genes show a smaller change or no change at all (**Supplementary Fig. 3** and **Supplementary Methods** online). It is not clear which of these changes (or which of their cumulative effects) influences C gene expression, and the possibility of translational inhibition of target gene expression[20,21] remains open. Thus, the questions of which *NF-YA* (or even how many) conveys the miRNA control to the C genes and precisely how *NF-YA* expression is controlled by miRBL or miRFIS will need to be addressed in the future.

Given that *FIS* is expressed in the center of the flower, but *fis* mutants do not show any detectable anomalies in stamen or carpel development, we asked if *FIS* is functional in the inner whorls. First, we tested *PLE* expression directly *in situ* by comparing serial longitudinal sections of wild-type and *fis* flowers at early developmental stages, when *PLE* transcription becomes detectable. *PLE* expression was enhanced in *fis* flowers (**Fig. 4**), demonstrating that miRFIS dampens *PLE* expression within the genuine C domain from the early stages onward. Furthermore, the domain of *PLE* expression is slightly broader in the *fis* mutant, as indicated by the presence of a hybridization signal farther from the center of the meristem than is found in the wild type (**Fig. 4a**,**f**).

To see if these expression changes have functional significance, we tested *A. majus* mutants with reduced C gene expression to determine if this could be overcome by removal of *FIS* activity (**Fig. 5**). In *fimbriata* (*fim*) mutants, expression of the B and C function genes is low and delayed[22]. Consequently, *fim* flowers resemble double mutants of B and C genes in that sepals are the only organ type that can readily develop (**Fig. 5a**,**d**). In the *fim fis* double mutant, carpel development is fully restored, and the central female organ incorporates carpels formed in the second and third whorls (**Fig. 5c**,**f**). Thus, *fim fis* recapitulates the *fis* phenotype with respect to carpel development, confirming the wild-type function of *FIS* as a repressive modulator of C function in the central whorls. Notably, the contribution of *fis* to enhanced C function in *fim* flowers is dosage dependent, as *fim* plants heterozygous for *fis* produce flowers with carpels in their third whorl, whereas sepals develop in their second whorl without carpel identity (**Fig. 5b**,**e**). Differential dosage dependence in the second whorl versus the inner whorls indicates that a threshold C expression level must be reached to initiate carpel morphogenesis; this is more readily accomplished in the central region, where the C function is activated and subsequently maintained, probably by autoregulation[23].

In the *fis* and *bl* mutants, the elevation of C gene expression in their genuine expression domains seems not to have any deleterious consequences, calling into question the developmental significance of the suppression mechanism in those tissues. One obvious possibility is that elevated C function in the inner whorls of the miRNA mutants confers ectopic C activity on the second whorl. This can happen only during the early stages when cells in which C genes are activated divide and can transmit C gene products to daughter cells. The result is a radial gradient of C gene expression, and the outward extension of this gradient depends on when and where the C expression for autoregulatory maintenance passes its threshold value. This then determines the extent of the region where organ

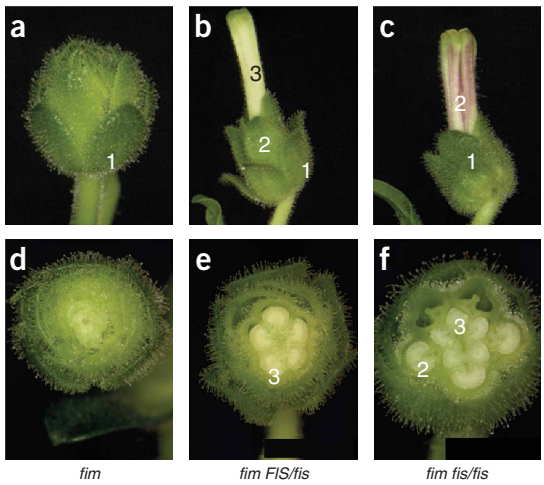

Figure 5 Rescue of organ identity defects of the *fim* mutant in the absence of miRFIS. (**a**–**f**) In the *fim* mutant (**a**,**d**), the B and C organ identity functions are impaired, and the flowers have sepals. In the *fim* background, reduction of the *FIS* dosage (**b**,**e**) and its complete absence (**c**,**f**) result in different degrees of ectopic carpel development. **d**–**f** are transverse sections showing the inner organs. For simplicity, C and B function–dependent defects in the organization of whorls and termination of flower development in *fim* mutants[6,10] are not considered in this report. Whorls are numbered, and genotypes are indicated.

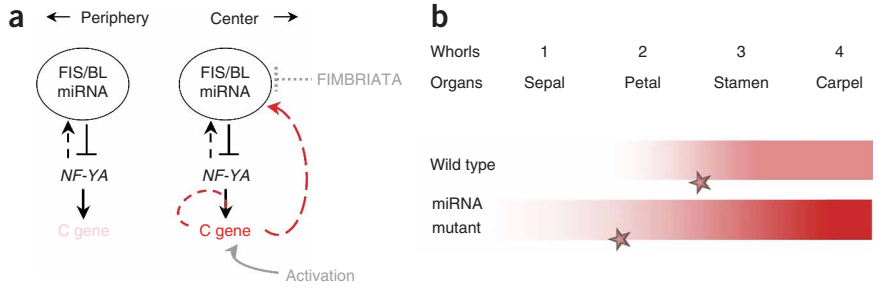

Figure 6 Regulatory mechanism governed by miRFIS and miRBL to maintain the C domain boundary by controlling early C gene expression. (**a**) Model illustrating the regulatory mechanism during C gene activation (gray) and immediately after C gene activation (black) in the wild-type flower. FIMBRIATA is a transiently expressed F-box protein[22] that temporarily antagonizes miRFIS. Feedback regulation of the *MIR* genes by the C genes is postulated to keep C gene expression at a desired level; fine-tuning is achieved by a feedback loop between the *MIR* genes and their direct target (*NF-YA*). Red lines indicate threshold-dependent activities governed by the C function. Arrows indicate activation, and barred lines indicate inhibition. Solid lines show direct regulatory relations, dotted lines show indirect events and dashed lines show hypothetical events. The positions of the floral whorls are indicated by numbers, with wild-type organs indicated under the numbers. (**b**) The bars shaded in red highlight the result of the regulatory circuit in adjusting C expression in the wild type and in the mutants. In the mutants, the miRNA-governed fine-tuning control is impaired, and early C gene expression increases primarily within the domain where C genes are activated. Lateral extension of the domain results from transmitting an excess of C gene products to daughter cells during cell divisions, reinforced by threshold-dependent autoregulation. Stars mark the threshold C function level above which C gene autoregulation takes place and the organ identity control is realized.

identity control can be exerted by C function. In the wild type, this coincides with the boundary between the third and the second whorl, but owing to the enhanced central C expression in the *MIR* mutants, the functional domain will expand into the second whorl (**Fig. 6**). In support for the postulated gradient of C gene expression, late *PLE* transcription in *fis* second whorl primordia is detectable in the adaxial region near the central domain but hardly ever in the first whorl[4,5], in agreement with the weakness or lack of homeotic conversion of sepals in the *fis* (or *bl*) mutants. The proposed simple dynamic mechanism readily reflects the wild-type and the miR mutant phenotypes and also accounts for the necessity of dampening C gene expression within the genuine functional domain, as observed in our experiments. A threshold-dependent feedback relationship between the C genes and the miRNAs would further balance the determination of the different primordia in space and time (**Fig. 6a**).

Taken together, our observations suggest an unusual miRNA-mediated mechanism in *P. hybrida* and *A. majus* for the control of the expression pattern of a floral homeotic gene. Instead of a spatially restricted 'clearing function', we observe a threshold-dependent adjustment of expression of the ultimate targets (the C genes) necessary to prevent their ectopic expression. The quantitative rather than qualitative nature of this control, which apparently bears a homeostatic aspect, is corroborated by the sensitivity of the regulatory event to *MIRFIS* dosage.

Components of the miRNA-governed control of C expression (such as *AtmiR169*, *NF-YA* genes and the respective *cis*-acting element in *AG*) exist in *A. thaliana*[17], but some elements of the early regulatory circuit mediated by miRBL and miRFIS in *P. hybrida* and *A. majus* are missing. For instance, although *FIM* antagonizes *FIS*, the *A. thaliana* ortholog of *FIM*, *UFO*, does not have any role in the positive control of early *AG* expression[24]. Therefore, it is likely that other mechanisms govern early adjustments of C expression in *A. thaliana*. Such differences in mechanistic details in early control processes in different species are also suggested by the lack of influence of *AP2*-like genes on C function in *P. hybrida* and *A. majus*, as mentioned before. Notably, the function of the transcription factor AP2 in *A. thaliana* is negatively modulated by an miRNA, *AtmiR172* (ref. 20). As in the miR169/*NF-YA* pairs, the *P. hybrida* and *A. majus AP2* orthologs also contain the recognition site for miR172 (ref. 25), and miR172 is conserved from ferns to higher plants[1]. The function of miR172 has not been assessed in *P. hybrida* and *A. majus*, but in a phylogenetically related species, *Nicotiana benthamiana*, the miR172/AP2 module does not seem to have a role in C gene control comparable to that in *A. thaliana*[26]. It seems, then, that the regulatory role of these two conserved miRNA/target modules in flower development diverged without major impact on the overall homeotic control of floral organ identity. Thus, target genes can shift in function while maintaining their miRNA/MRE relationship.

METHODS

Plant material. The origin of the *fis*-1 and *fim* (*fim*-679) mutants and the wild type, as well as cultivation methods, have been described elsewhere[5,22]. *fis*-2 appeared spontaneously in a segregating F_2 population after a cross of two unrelated *A. majus* lines. *bl*-1 was originally obtained from the Sluis and Groot seed company; *bl*-2 arose spontaneously during propagation of recombinant inbred lines (see Acknowledgments).

5′ RACE. Total RNA from *A. majus* inflorescences was isolated with the RNeasy Maxi Kit (Qiagen), and polyA$^+$ RNA was obtained using magnetic beads (Dynabeads Oligo(dT)$_{25}$, Invitrogen). To determine the 5′ end of the *MIRFIS* transcript (pri-*MIRFIS* in **Fig. 2a**), the SMART procedure (Clontech) was applied; PCR amplification was performed with the SMART 5′ oligonucleotide and a reverse primer derived from the pre-*MIRFIS* stem-loop structure (**Supplementary Table 2** online). The resulting fragments were subcloned into the pGEMt vector (Promega), and four recombinant plasmids were sequenced.

Cloning strategies. Construction of the *A. majus* BAC library and map-based cloning by chromosome walking will be described elsewhere. For the cloning of *BL*, we used a transposon-display strategy[27]. *FIS* was identified by applying the Universal Genome Walker kit (BD Biosciences) using sequence information derived from the *BL* DNA sequence and testing BACs from the wild-type region spanning the deletion in the *fis*-1 genome with the obtained fragments. The ultimate proof of locus identity came from sequencing PCR-amplified genomic regions from wild-type revertants of the genetically unstable *bl*-2 and *fis*-2 alleles.

cDNA clones for *AmNF-YAs* were obtained by screening a normalized λNM1149 cDNA library with *A. thaliana* probes obtained by RT-PCR amplification on *A. thaliana* first-strand cDNA using primers specific for individual *AtNF-YAs*. For isolation of *PhNF-YAs*, RT-PCR was performed on *P. hybrida* first-strand cDNA with degenerate primers Ph-YF1 or Ph-YF2 derived from the C-terminal highly conserved region[15] and the miRBL MRE (Ph-YR; see **Supplementary Table 2**). For a phylogenetic tree constructed with these sequences and for the nomenclature, see **Supplementary Figure 1**.

***In situ* hybridization.** The locked nucleic acid (LNA)-modified digoxigenin-labeled antisense oligonucleotide probes listed in **Supplementary Table 2a** were obtained from Exiqon and used for hybridization on 10-μm tissue sections as described[28]. Optimal concentrations and hybridization temperatures were determined independently for each probe. For tissue preparation and

hybridization with conventional digoxigenin-labeled probes, see refs. 8,10. The specificity of the miRNA probes was confirmed by the lack of a reliable signal probing *bl*-1, *fis*-1 (**Fig. 3a**,**b**) and *fis*-2 sections, and the difference in miRNA expression between wild-type and mutant floral buds was corroborated by miRNA gel blots (**Supplementary Fig. 3**). *In situ* hybridization with the shorter miR169 core probe produced signals in the mutants in a pattern similar to that of *BL* and *FIS* in the wild type, confirming expression of other miR169 family members in *P. hybrida* and *A. majus* (data not shown). Specificity of the *AmYA2* and *AmYA4* LNA-modified probes was corroborated by hybridizations with the respective conventional probes, which yielded identical patterns but very low signal intensity (**Supplementary Fig. 2**). Images were captured under bright-field illumination with a Zeiss Axiophot microscope equipped with plan-NEOFLURAL objectives, a JVC KY-F70 digital camera and Discus software and were processed equally for background subtraction with Adobe Photoshop.

Accession codes. EMBL Nucleotide Sequence Database: *A. majus NF-YA* cDNA sequence: AM422770–AM422775; *P. hybrida* NF-YA cDNA sequence: AM489758–AM489763; *FIS* gene: AM422776; *BL* gene AM489765.

Requests for materials: schwarzs@mpiz-koeln.mpg.de

Note: Supplementary information is available on the Nature Genetics website.

ACKNOWLEDGMENTS

We thank J. Burgyan for information on *in situ* analyses with miRNA; J. Stuurman and J. Moore (University of Berne) for the *bl*-2 allele and B. Davies, P. Huijser, H. Saedler and P. Schulze-Lefert for discussions and comments. This work was supported in part by a grant from the Deutsche Forschungsgemeinschaft/SFB572 (Z.S.-S.).

AUTHOR CONTRIBUTIONS

All authors contributed to the experiments, which were conceptually designed mainly by M.V. and Z.S.-S. Z.S.-S. wrote the manuscript, with support from M.V., M.C. and T.G.

COMPETING INTERESTS STATEMENT

The authors declare no competing financial interests.

Published online at http://www.nature.com/naturegenetics/
Reprints and permissions information is available online at http://npg.nature.com/reprintsandpermissions

1. Axtell, M.J. & Bartel, D.P. Antiquity of microRNAs and their targets in land plants. *Plant Cell* **17**, 1658–1673 (2005).
2. Baulcombe, D. RNA silencing in plants. *Nature* **431**, 356–363 (2004).
3. Vallade, J., Maizonnier, D. & Cornu, A. La morphogenese florale chez le petunia. I. Analyze d'un mutant à corolle staminée. *Can. J. Bot.* **65**, 761–764 (1987).
4. McSteen, P.C.M., Vincent, C.A., Doyle, S., Carpenter, R. & Coen, E.S. Control of floral homeotic gene-expression and organ morphogenesis in *Antirrhinum*. *Development* **125**, 2359–2369 (1998).
5. Motte, P., Saedler, H. & Schwarz-Sommer, Z. *STYLOSA* and *FISTULATA*: regulatory components of the homeotic control of *Antirrhinum* floral organogenesis. *Development* **125**, 71–84 (1998).
6. Davies, B., Cartolano, M. & Schwarz-Sommer, Z. Flower development: The *Antirrhinum* perspective. *Adv. Bot. Res. Inc. Adv. Plant Pathol.* **44**, 278–319 (2006).
7. Jack, T. Molecular and genetic mechanisms of floral control. *Plant Cell* **16**, S1–S17 (2004).
8. Navarro, C. *et al.* Molecular and genetic interactions between STYLOSA and GRAMINIFOLIA in the control of *Antirrhinum* vegetative and reproductive development. *Development* **131**, 3649–3659 (2004).
9. Kater, M.M. *et al.* Multiple AGAMOUS homologs from cucumber and petunia differ in their ability to induce reproductive organ fate. *Plant Cell* **10**, 171–182 (1998).
10. Davies, B. *et al. PLENA* and *FARINELLI*: redundancy and regulatory interactions between two *Antirrhinum* MADS-box factors controlling flower development. *EMBO J.* **18**, 4023–4034 (1999).
11. Maes, T. *et al. Petunia* Ap2-like genes and their role in flower and seed development. *Plant Cell* **13**, 229–244 (2001).
12. Keck, E., McSteen, P., Carpenter, R. & Coen, E. Separation of genetic functions controlling organ identity in flowers. *EMBO J.* **22**, 1058–1066 (2003).
13. Jones-Rhoades, M.W., Bartel, D.P. & Bartel, B. MicroRNAs and their regulatory roles in plants. *Annu. Rev. Plant Biol.* **57**, 19–53 (2006).
14. Xie, Z. *et al.* Expression of *Arabidopsis* MIRNA genes. *Plant Physiol.* **138**, 2145–2154 (2005).
15. Gusmaroli, G., Tonellia, C. & Mantovani, R. Regulation of the CCAAT-Binding NF-Y subunits in *Arabidopsis thaliana*. *Gene* **283**, 41–48 (2002).
16. Schwab, R. *et al.* Specific effects of microRNAs on the plant transcriptome. *Dev. Cell* **8**, 517–527 (2005).
17. Hong, R.L., Hamaguchi, L., Busch, M.A. & Weigel, D. Regulatory elements of the floral homeotic gene *AGAMOUS* identified by phylogenetic footprinting and shadowing. *Plant Cell* **15**, 1296–1309 (2003).
18. Nikovics, K. *et al.* The balance between the *MIR164A* and *CUC2* genes controls leaf margin serration in *Arabidopsis*. *Plant Cell* **18**, 2929–2945 (2006).
19. Hornstein, E. & Shomron, N. Canalization of development by microRNAs. *Nat. Genet.* **38**, S20–S24 (2006).
20. Chen, X. A microRNA as a translational repressor of *APETALA2* in *Arabidopsis* flower development. *Science* **303**, 2022–2025 (2004).
21. Gandikota, M. *et al.* The miRNA156/157 recognition element in the 3′ UTR of the *Arabidopsis* SBP box gene SPL3 prevents early flowering by translational inhibition in seedlings. *Plant J.* **49**, 683–693 (2007).
22. Ingram, C.G. *et al.* Dual role for *fimbriata* in regulating floral homeotic genes and cell division in *Antirrhinum*. *EMBO J.* **16**, 6521–6534 (1997).
23. Gomez-Mena, C., de Folter, S., Costa, M.M.R., Angenent, G.C. & Sablowski, R. Transcriptional program controlled by the floral homeotic gene *AGAMOUS* during early organogenesis. *Development* **132**, 429–438 (2005).
24. Ingram, G.C. *et al.* Parallels between *unusual floral organs* and *fimbriata*, genes controlling flower development in *Arabidopsis* and *Antirrhinum*. *Plant Cell* **7**, 1501–1510 (1995).
25. Shigyo, M., Hasebe, M. & Ito, M. Molecular evolution of the AP2 subfamily. *Gene* **366**, 256–265 (2006).
26. Mlotshwa, S., Yang, Z., Kim, Y. & Chen, X. Floral patterning defects induced by *Arabidopsis APETALA2* and microRNA172 expression in *Nicotiana benthamiana*. *Plant Mol. Biol.* **61**, 781–793 (2006).
27. Van den Broeck, D. *et al.* Transposon display identifies individual transposable elements in high copy number lines. *Plant J.* **13**, 121–129 (1998).
28. Valoczi, A., Varallyay, E., Kauppinen, S., Burgyan, J. & Havelda, Z. Spatio-temporal accumulation of microRNAs is highly coordinated in developing plant tissues. *Plant J.* **47**, 140–151 (2006).

Supplementary Table 1: Position of cleavage sites in the MRE of Antirrhinum and Petunia NF-YA transcripts*

NF-YA target	cleavage site position	number of clones analyzed
PhYA1	10/11	6
PhYA2	10/11; 13/14	3 (2;1)
PhYA3	10/11	4
AmYA1	10/11	4
AmYA2	10/11	3
AmYA3	10/11	2
AmYA4	10/11	3

*see Supplementary methods for details of the 5' RLM-RACE

Supplementary Table 2: Oligonucleotide sequences

A. RT-PCR and in situ hybridizations

Designation	Oligonucleotide sequence (5'-3')	REMARKS
Ph-YF1	GAACCAGTTTWTGTTAATGC	RT-PCR primers for cloning PhNF-YAs
Ph-YF2	GARCCWATNTWTGTNAATGC	
Ph-YR	AGCCAAGRATGAATTGCC	
FIS	CGTCGGCAAGTCATCCTTGGCTATA	LNA modified oligonucleotides for in situ analyses
BL	TGCCGGCAAGTCATCCTTGGCTGC	
AmYA2	GATGATCTGCCAGTT	
AmYA4	AATGAATTGCCGCCC	
pre-miRFIS	ACTTACTTTCGTCGGCAAGTCATCCTTGGC	5'-RACE

B. 5'RLM-RACE

Gene	Reverse primer	Nested reverse primer
Ph-YA1	5'-TCTCAAAACACCACAACAGTAGTCC-3'	5'-CCAAACACACTGCATCATTACAGAC-3'
Ph-YA2	5'-CAGAGCAATACAAAGCACATGAGGA-3'	5'-AGGAGAAAATGGCCTCAACTCCAC-3'
Ph-YA3	5'-AGCCAATCCACAAATAGCCACAC-3'	5'-AGCCACACAATCAAAATGCTGCAG-3'
Am-YA1	5'-CAAACTTCAAGACATCAGCACCGTACC-3'	5'-ATTTCACATGACAGAACTGCACAGT-3'
Am-YA2	5'-GGATAGATTGCAGAGGACTACATACC-3'	5'-CAGAATTTATGTTCAAGTGCAGGTTC-3'
Am-YA3	5'-CCTATGAATCACAATCTCACATACTGTCAC-3'	5'-GAACCCACACAGAAGTTTACAGACAG-3'
Am-YA4	5'-CATGCTAAATCCGACAGAAACTCAAG-3'	5'-GCAACGACATAACCCACTCAAACTCG-3'

C. Quantitative RT-PCR

Gene	Forward primer	Reverse primer
Ph-YA1*	5'-TACTGGACATGGTATTCTC-3'	5'-CATTGATAGCCAAGGATG-3'
Ph-YA2**	5'-TTACAAGCATCTTCAGTGG-3'	5'-GATAACACAAACACACAGTC-3'
Ph-YA3*	5'-ACAAAGGACACAGCCATAG-3'	5'-CCATTCCCTTGCTCATTTC-3'
Ph-YA4*	5'-TCTTATTCAAACGGTAGCAG-3'	5'-AGTTCAAGAGCCGATTTAG-3'
Ph-YA5*	5'-TCTGCTTTCTCAAGTGTC-3'	5'-TGTCTTTGCCAGTTAGG-3'
Ph-YA6**	5'-CTACCATCAGCAATCACTC-3'	5'-TGTTGAGGTCGTTCTTCC-3'
PMADS3**	5'-TTCTTGGTGAATCTCTTGCTG-3'	5'-GGTAATGGTTGTTGGTCTGC-3'
Ph-Actin**	5'-GTTGGACTCTGGTGATGGTGTG-3'	5'-CCGTTCAGCAGTGGTGGTG-3'
pri-BL*	5'-CATCAAAATTCTGGCATGAG-3'	5'-GCAAGCTTGATCAACTCTAC-3'

* primer annealing temperature = 62°C; ** primer annealing temperature = 58 °C

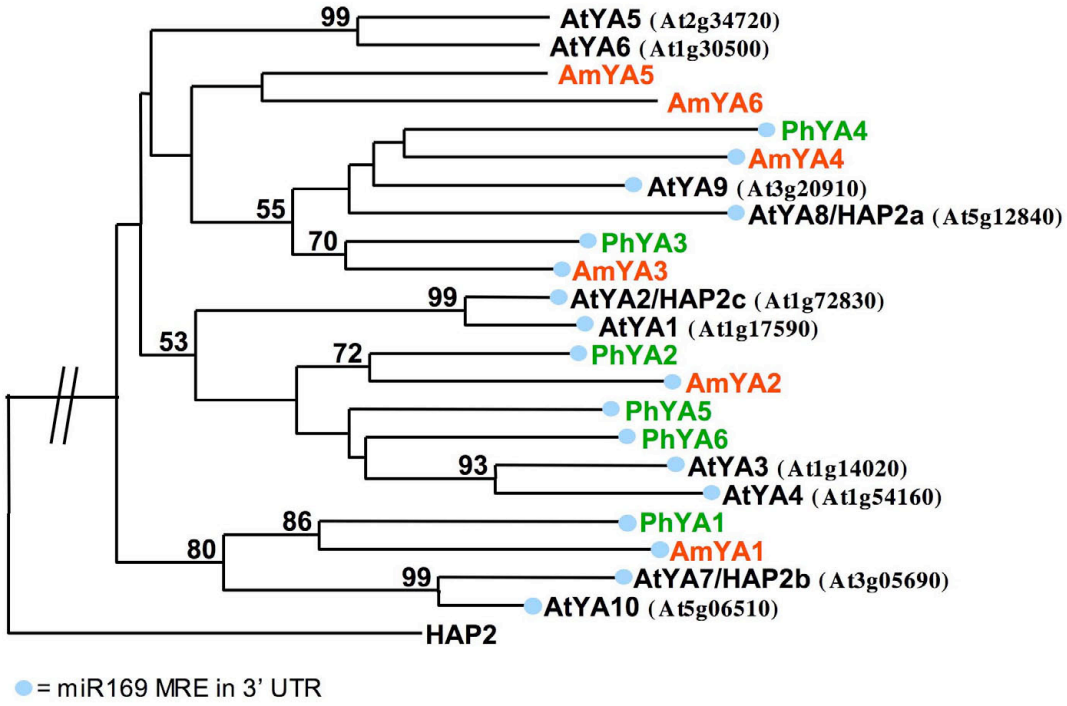

Supplementary Figure 1 Neighbor-Joining Tree of Antirrhinum, Petunia and Arabidopsis NF-YA family members. For phylogenetic analysis the cDNA sequence of a conserved region residing within the DNA-binding domain of the NF-YA sequences from Petunia, Antirrhinum and Arabidopsis were aligned using CLUSTAL W and edited using BioEdit (http://www.mbio.ncsu.edu/BioEdit/bioedit.html). A neighbour-joining tree was computed using the Treecon programme (Van de Peer and Wachter, 1994); 1000 bootstrap samples were generated to support the inferred relationships and HAP2 from yeast (M15243) was used to root the tree. Antirrhinum sequences are shown in red, Petunia sequences are in green, and Arabidopsis sequences are in black (numbered according to[17]). Local bootstrap probabilities above 50% are shown near the major branching points.

Van de Peer, Y. & De Wachter, R. TREECON for Windows: a software package for the construction and drawing of evolutionary trees for the Microsoft Windows environment. *Comput. Appl. Biosci.* **10**, 569-570 (1994).

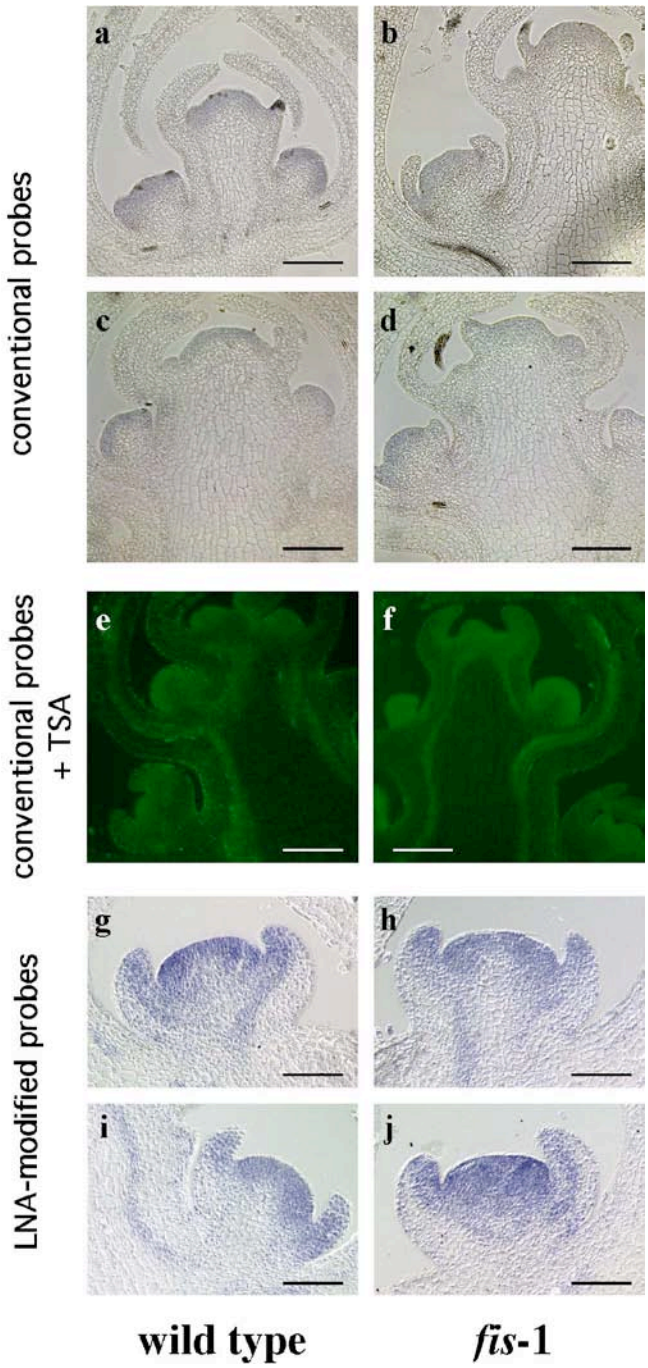

Supplementary Figure 2 Detection of the in situ expression patterns of Antirrhinum *NF-YA* genes by different methods. Wild-type and *fis*-1 mutant inflorescences were hybridized with a DIG-labeled antisense RNA probe derived from the full-size AmYA2 (**a, b, e, f,**) and AmYA4 (**c, d,**) cDNAs. In **e, f,** the Tyramide Signal Amplification (TSA) Fluorescein technology (Perkin Elmer Life Sciences Inc.) was used for signal enhancement. These experiments were performed to investigate the specificity of the signals obtained with the AmYA2 (**g, h,**) and AmYA4 (**i, j**,) LNA probes (also see Fig. 3). Bar in a-f = 200μm and in g-j = 100μm

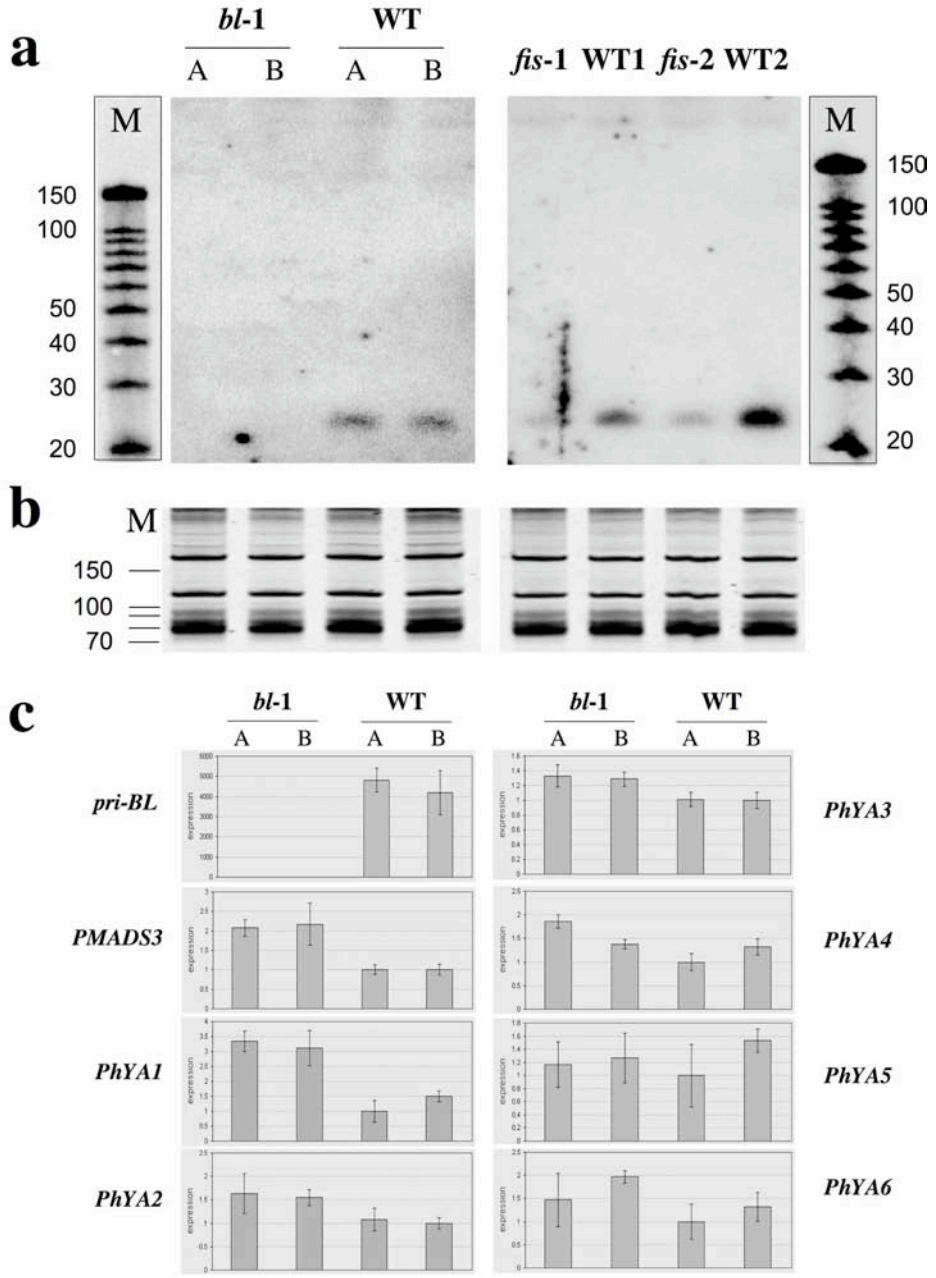

Supplementary Figure 3 **a, b, RNA blot analysis of microRNA expression**. **a**, 15 µg of total RNA prepared of young Petunia (left panel) and Antirrhinum flower buds (right panel) with genotypes indicated above the lanes was loaded on a denaturing 15% polyacrylamide gel. After transfer to nylon membranes the blot was hybridized with a 5' end-labeled LNA probe (sequence as shown in the Methods for in situ experiments) as recommended by Exiqon. M = RNA decamere size marker; A and B are two biological replicas for wild-type and *bl* Petunia buds; WT1 and WT2 are two different wild-type lines representing the genetic background for *fis*-1 and *fis*-2. **b**, 1 µg of total RNA was loaded on an ethidium bromide-stained 15% polyacrylamide gel to control equal loading. **c, Analysis of gene expression by qRT-PCR**. First strand cDNA prepared on the Petunia total RNA templates used for the analyses shown in a,b, was subjected to qPCR with primers amplifying gene products as indicated. The y-axes show fold expression with respect to the lowest value in a series; bars represent standard deviation of three independent PCR experiments.

Supplementary Methods.

5' RLM-RACE. The Ambion FirstChoice® RLM-RACE Kit was applied to polyA$^+$ RNA to determine the 5' end of the NF-YA cleavage products[18] (Supplementary Table 1). For the final PCR reaction the nested gene-specific primer (Supplementary Table 2B) was 5' end-labeled and for cloning in the pGEMt vector the PCR products were excised after electrophoretic separation on a 4.5% polyacrylamide gel.

qRT-PCR. Quantitative real-time RT-PCR analysis was performed in a MyiQ real-time PCR machine (BioRad) as described (Rijpkema et al., 2006). For cDNA synthesis total RNA was prepared from two independently pooled samples of young floral buds collected from different plant individuals. Expression values were normalized against actin. The primers used in this assay are listed in Supplementary Table 2C.

Rijpkema, A. S. et al. Analysis of the Petunia TM6 MADS box gene reveals functional divergence within the DEF/AP3 lineage. *Plant Cell* **18**, 1819-1832 (2006).